IONIC MASS TRANSFER WITH SUBMERGED JETS-I

(CORRELATION OF THE DATA IN THE IMPINGEMENT REGION)

By

B. SUBBA RAO, M. S. KRISHNA* and G. J. V. JAGANNADHA RAJU

Department of Chemical Engineering, Andhra University, Visakhapatnam, India

Received 8, September 1971

Fluid jets are used to provide high transfer rates. The previous studies [1—4] with fluid jets were confined to heat transfer or mass transfer associated with either dissolution or sublimation of substances. In view of the numerous parameters involved, the problem has become extremely complex and thus impeded theoretical treatment.

According to RAO and TRASS [2], a jet of liquid impinging normal to the surface can be divided into four flow regions: the transition jet region, the fully developed jet region, the impingement region and the wall-jet region. The former two regions refer to flow characteristics of the jet while the latter two refer to the flow on the target area. Many investigators observed the two regions on the target surface although there was no concurrence on the quantitative values of the boundaries of these regions. The present investigation is directed towards a systematic study of mass transfer at concentric ring electrodes on the target area. The work reported in this paper is a part of the study with submerged jets and confines to the radial variation of mass transfer coefficients on the target surface and the correlation of the data in the impingement region.

Experimental

The equipment used in the present study is shown in Fig. 1. It essentially consisted of a copper storage drum, a centrifugal pump for circulating the electrolyte, rotameters for measuring the flow of the electrolyte, a double pipe arrangement for adjusting the height of the nozzle and an electrolytic cell containing the ring electrodes on the bottom surface of the cell.

The electrolyte from the storage tank was pumped through the rotameters before it entered the nozzle assembly. The arrangement for adjusting the nozzle to any desired height is shown in Fig. 2. With suitable sizes of

* Present address: Department of Chemical Engineering, Coimbatore Institute of Technology, Coimbatore—14. India

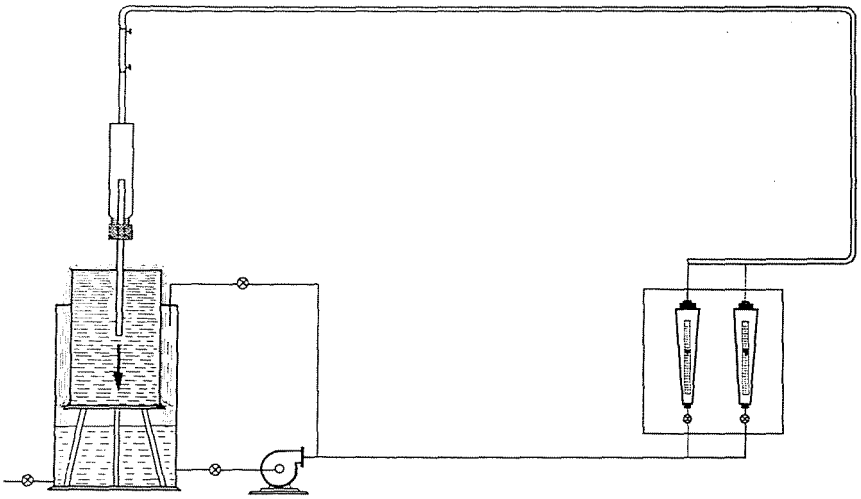

Fig. 1. Schematic diagram of the Equipment

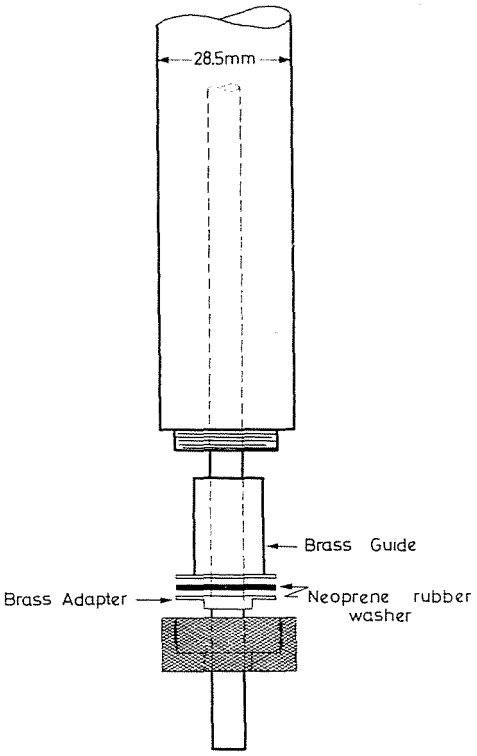

Fig. 2. Detailed drawing of the nozzle-sleeve arrangement

adapters, three sizes of nozzles 251, 15.8 and 9.4 mm i.d. could be used. While mounting the nozzle into the assembly, care was taken to fix the nozzle axi-symmetric to the electrolytic cell.

The electrolytic cell is shown in Fig. 3. It is the same as the one used in the earlier studies on stirred tanks [5]. It essentially consisted of a bottom plate made from laminated phenyl formaldehyde resin, and a copper cylindrical cell. The bottom plate was provided with sixteen electrodes in the form of

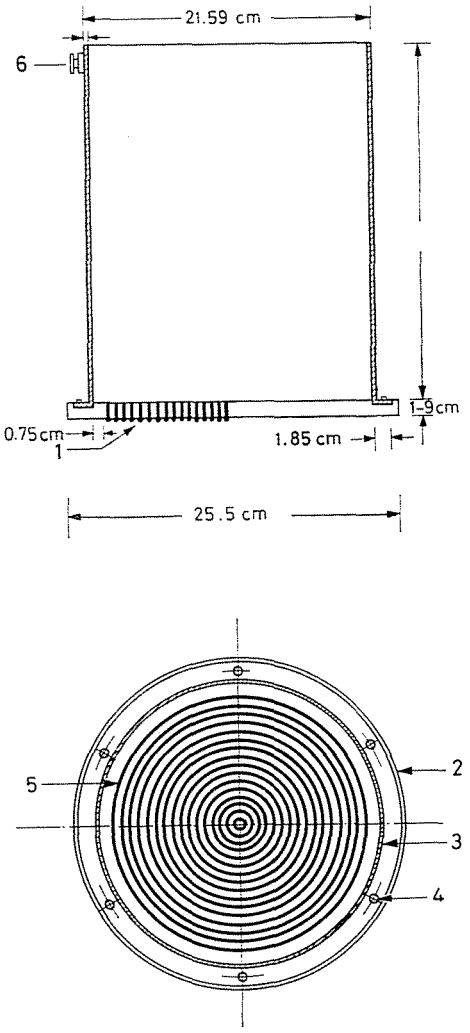

Fig. 3. Detailed drawing of the Electrolytic cell. 1. Electrical connections, from sixteen ring electrodes; 2. Hylam bottom plate with copper ring electrodes fixed flush with it; 3. Copper cylindrical shell; 4. Holes for fixing nuts and bolts; 5. Copper ring electrodes (sixteen in all); 6. Plug for outer wall-electrode

concentric rings and were fixed flush with the surface of the plate and the electrical connections to the electrodes protruded from the bottom of the plate. The dimensions of the electrodes are given in Table 1. The electrolytic cell was mounted on a ring of a tripod stand which was in turn installed in the storage tank. The entire assembly is fixed rigidly to avoid vibrations resulting from the impinging electrolyte. The level of the electrolyte in the storage tank

Table 1

Details of the electrolytic cell
Diameter of the vessel D: 21.59 cm

Ring No.	Mean dia. cm	Width of the ring t, cm	Gap widht $(d - d_m)/2$ cm
1.	19.211	0.714	1.190
2.	18.003	0.786	1.793
3.	16.604	0.746	2.493
4.	15.303	0.750	3.144
5.	14.042	0.696	3.774
6.	12.754	0.688	4.418
7.	11.490	0.712	5.050
8.	10.229	0.694	5.681
9.	8.992	0.716	6.299
10.	7.786	0.700	6.902
11.	6.638	0.656	7.476
12.	5.469	0.718	8.065
13.	4.294	0.676	8.648
14.	3.084	0.726	9.250
15.	1.914	0.712	9.838
16.	0.681	0.614	10.450

Table 2

Range of variables covered

Variable	Minimum	Maximum	Max/Min
Diameter of the nozzle, cm	0.94	2.51	2.671
Height of the nozzle above the plate, cm	7.63	23.30	3.054
Mean diameter of the ring electrode, cm	0.681	19.21	28.21
Velocity of the submerged impinging jet, m/s	0.4781	7.844	16.41
Reynolds number (based on the diameter of the nozzle)	6.680	109.858	16.44

was maintained well below the bottom plate of the test cell. The cell was provided with a copper sheet deflector to prevent the overflowing electrolyte from contacting the electrical contact points.

The system used for the study is the reduction of ferricyanide ion. Equimolar solution of potassium ferrocyanide and potassium ferricyanide (1×10^{-5} g moles/ml) with excess indifferent electrolyte (0.5 N sodium hydroxide) is used as the electrolyte. The experimental and the analytical procedures are similar to those adopted in the previous studies [5—7].

Results

The variables investigated are compiled in Table 2. The mass transfer coefficients were evaluated in the customary manner [5—7] from the measured limiting current densities and the concentration of the electrolyte as:

$$K_L = I/zFc_0 \tag{1}$$

The previous studies with jets indicate that the mass transfer coefficient is a function of flow rate of the fluid, the relative distance of the nozzle from the plate, the diameter ratio and the physical properties of the electrolyte.

In order to correlate the present data, it would be logical as initial step to investigate the effect of the different operating variables on the mass transfer coefficient at various electrodes. It is also necessary to establish the boundaries of the so called impingement and wall-jet regions, in terms of the radial distance x or the mean diameter of the ring electrode, d_m.

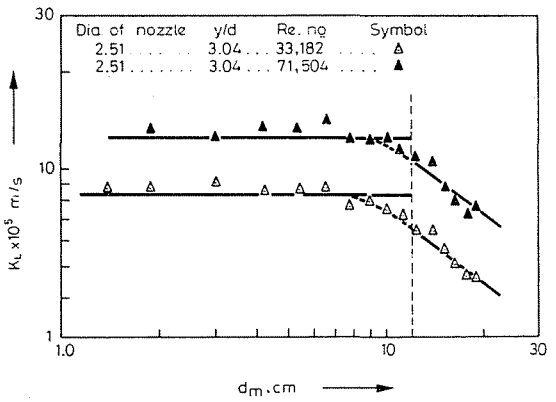

Fig. 4a. Variation of mass transfer coefficient with mean dia. of rings. 2.51 dia. nozzle

In Fig. 4a, mass transfer coefficients obtained at various flows with 2.51 cm nozzle located at a height of 7.62 cm above the plate are plotted against the mean diameter of the ring d_m. The values of the mass transfer coefficients show the existence of two distinct regions. For each flow rate, beyond a certain value of the mean ring diameter, the mass transfer coefficient decreases

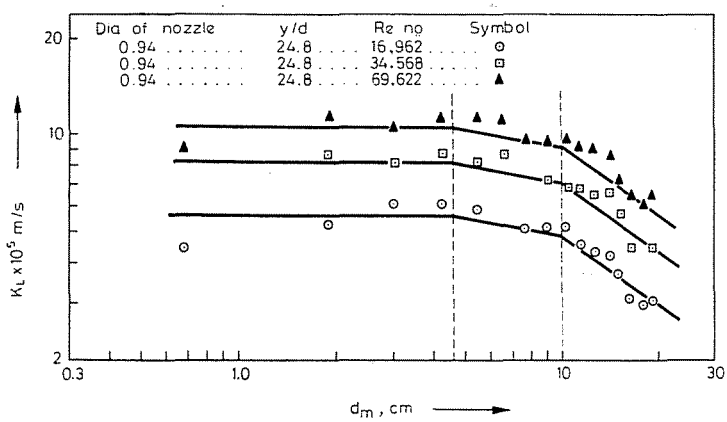

Fig. 4b. Variation of mass transfer coefficient with mean dia. of rings. 0.94 dia. nozzle

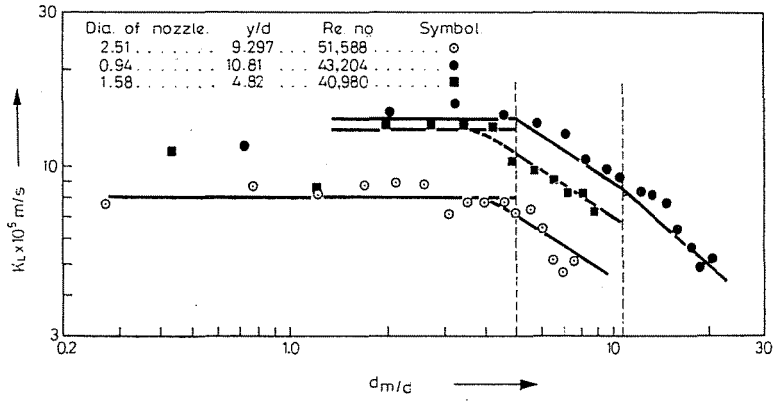

Fig. 5. Variation of mass transfer coefficient with d_m/d

rapidly. A similar plot (4b) of the data for 0.94 cm diameter nozzle shows a different value for the mean ring diameter. Also in this case the so-called wall-jet region has shown two sub-regions which may be termed as the transition region and the fully developed wall-jet region. Thus, the boundaries of the regions depend also on the diameter of the nozzle.

In Fig. 5, mass transfer coefficients K_L, are plotted against d_m/d. Three regions, namely the impingement region, (d_m/d value from 0.44 to 5 or x/d

value from 0.22 to 2.5); transition wall-jet region (d_m/d value from 5 to 10.88 or x/d value from 2.5 to 5.44); and fully developed wall-jet region (d_m/d value from 10.88 to 28 and x/d value from 5.44 to 14) are apparent in these plots.

Correlation of data in the impingement region

The experimental data with three nozzles situated at four different heights above the target surface are shown in Fig. 6, Sh_{av} as a function of the Reynolds number. The plots in the figure reveal that an increase in the y/d

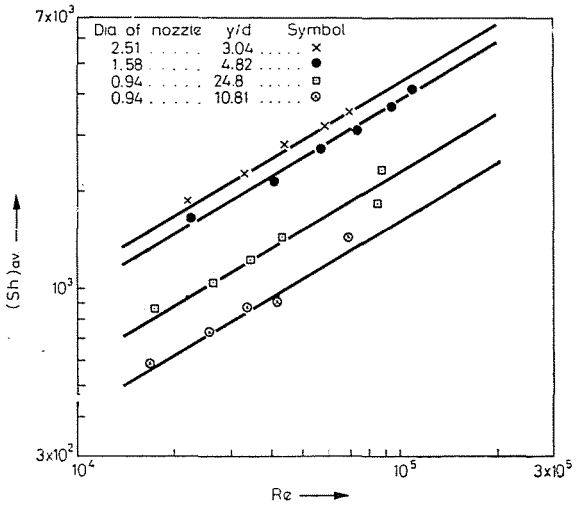

Fig. 6. $(Sh)_{av}$ as a function of Re for different nozzles situated at different heights

value results in a decrease in Sh_{av} and that in each case the Sh_{av} varies as $(Re)^{0.58}$. A cross plot for the plots in the figure at a Reynolds number of 70 000 is shown in Fig. 7. Sh_{av} is found to vary as $(y/d)^{-0.48}$.

All experimental data obtained in the impingement region are plotted in Fig. 8, as $Sh_{av}\,(y/d)^{0.48}$ vs. Re. The data are found to be correlated by the following dimensionless equation:

$$Sh_{av}(y/d)^{0.48} = 9.5(Re)^{0.58}. \qquad (2)$$

Except for a few runs the data have clustered together along the plot of Eq. (2).

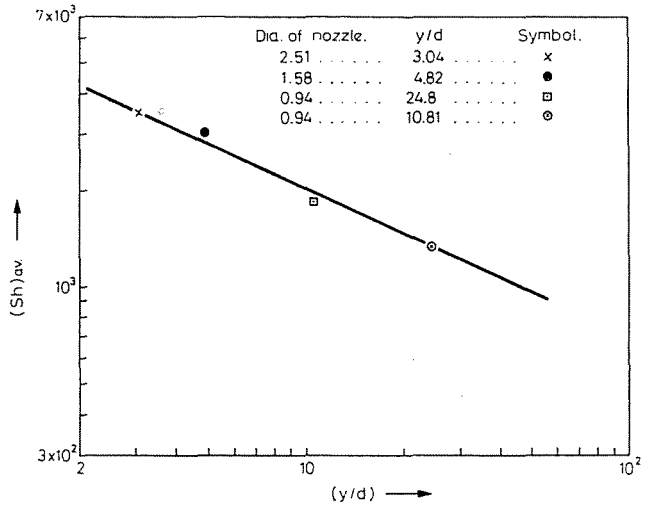

Fig. 7. Effect of (Y/d) on $(Sh)_{av}$

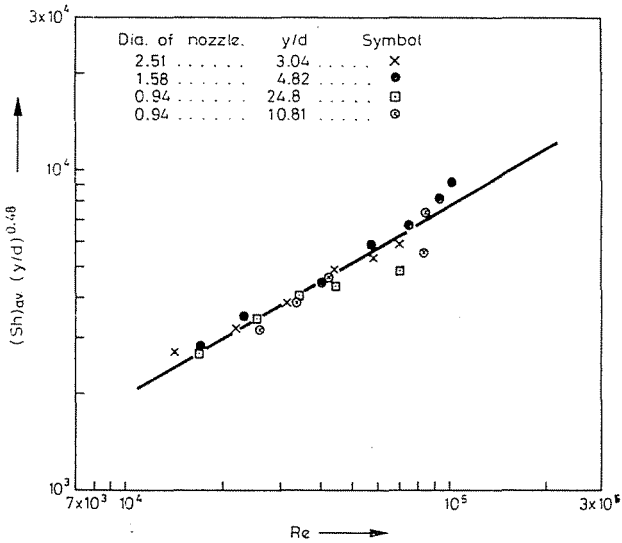

Fig. 8. Correlation plot of experimental data

In order to demonstrate the deviation between local and average *Sh* values, the Sh_{av} are plotted against *Sh* in Fig. 9. The maximum deviations of local from average Sherwood values are found to be within 15 per cent, the majority of the data being within 5 per cent. Therefore, Eq. (2) can also be used with a reasonable accuracy for predicting the local coefficient in the im-

pingement region of the submerged jet on the target area. In lack of precise knowledge on the effect of *Sc* group in the impingement region no attempt has been made to introduce this group into Eq. (2).

In their earlier investigation RAO and TRASS [2] proposed the following equation for correlating the mass transfer data in the impingement region:

$$Sh_{av} = 0.046(Re)^{1.06}(y/d)^{-0.09} \quad \text{for} \quad y/d < 6.5, \tag{2a}$$

$$Sh_{av} = 0.107(Re)^{1.06}(y/d)^{-0.54} \quad \text{for} \quad y/d \geq 6.5. \tag{2b}$$

SEETHARAMAYYA and SUBBA RAJU [4] correlated heat transfer data in the impingement region by the following equation:

$$Nu(Pr)^{-0.33} = 0.5077(Re)^{0.523}. \tag{3}$$

Comparison of Eq. (2) with Eqs (2a and 2b) and (3) reveals that they differ not only in the values of their constants but also in the functional dependence of Sh_{av} on y. Eq. (3) reveals that there is no effect of y while according to Eqs (2a and 2b), y is a variable, its effect being dependent on the y/d values. For values of $y/d < 6.5$, Sh_{av} is found to be a function of $y^{-0.09}$ and for values of $y/d \geq 6.5$, Sh_{av} varied as $(y)^{-0.54}$. The data of SEETHARAMAYYA and SUBBA RAJU [4] are in the range $y/d \leq 7.1$. In the present study, throughout the range of investigation in the impingement region Sh_{av} is found to vary as

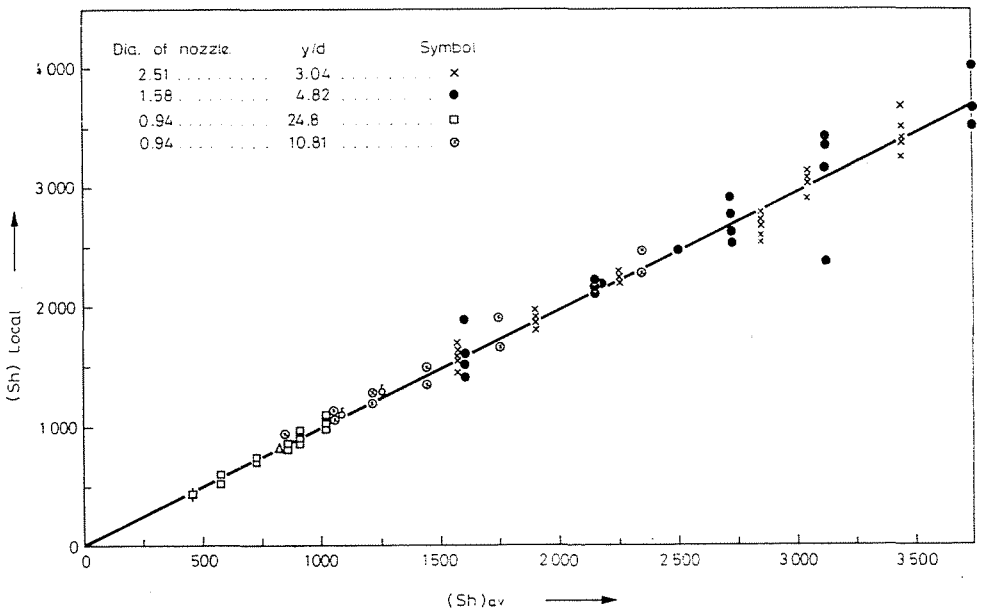

Fig. 9. Deviation of Local values from average *Sh* values

$(y)^{-0.48}$ although there is an eight-fold variation in y/d values, involving nozzle diameter variation from 0.94 to 2.51 cm and nozzle to plate distance from 7.63 to 23.3 cm. In these studies involving electrode reactions, the surface condition remains unaltered offering a better reproducibility of the data.

Conclusions

1. An increase in the velocity of the electrolyte increased the limiting current density and thereby the mass transfer coefficient.

2. At a given flow rate, the mass transfer coefficients at the sixteen electrodes show the existence of three distinct regions which may be termed as: (i) impingement region (ii) transition wall-jet region and (iii) fully developed wall-jet region.

3. The impingement region is characterized by nearly constant mass transfer coefficients and this region extends up to a d_m/d value of 5 (or x/d value 2.5).

4. The transition wall-jet region is characterized by a decrease in the mass transfer coefficients and this region corresponds to delete 5 to 10.88 d_m/d range.

5. The third region termed as fully developed wall-jet region is characterized by a rapid decrease of the mass transfer coefficients and the region corresponds to d_m/d values greater than 10.88.

6. In the impingement region an increase in the height of the nozzle (y) from the target surface results in a decrease in the value of mass transfer coefficient.

7. The following dimensionless equation is proposed for correlating the data in the impingement region: $Sh_{av}(y/d)^{0.48} = 9.5(Re)^{0.58}$.

Summary

Ionic mass transfer for the case of reduction of ferricyanide ion in presence of excess of indifferent electrolyte at the copper electrodes in the form of rings fixed flush with the surface of a flat plate held normal to the submerged jet of liquid was studied experimentally.

The experimental data indicate that the target area can be resolved into three regions viz., impingement region, transition wall-jet region and fully developed wall-jet region. An equation has been proposed for correlating the data in the impingement region.

Symbols

Co = concentration of the reacting ion in the bulk of the solution, g moles/ml.
D_L = coefficient of diffusion, cm²/sec.
d = diameter of the nozzle, cm.
d_m = mean diameter of the ring electrode, cm.
F = Faraday equivalent, 96,500 C/equivalent.
I = limiting current density, A/cm².

K_L = mass transfer coefficient, cm/sec.
K_{Lav} = average mass transfer coefficient, cm/sec.
z = number of electrons exchanged in the electrode reaction.
v = velocity based on the nozzle diameter, cm/sec.
x = mean radial distance of the ring electrode, cm.
y = distance of the bottom plate from the nozzle, cm.
p = density of the electrolyte, g/cm^3.
μ = viscosity of the electrolyte, g/cm/sec

Dimensionless parameters:

Re = dVp/μ = Reynolds number for flow through nozzle.
Sc = $p/\mu D_L$ = Schmidt number.
Sh = $K_L d/D_L$ Sherwood number.
Sh_{av} = $K_{Lav}\, d/D_L$, average Sherwood number.

References

1. Albertson, M. L., Dai, Y. B., Jonson, K. A. and Rouse, H.: Transactions of A.S.C.E. **115**, 639 (1950)
2. Rao, V. V. and Olev, Trass.: The Canadian J. Chem. Engg. **42**, 95 (1964)
3. Dawson, D. A. and O. Trass.: The Canadian J. Chem. Engg. **44**, 121 (1966)
4. Seetharamayya, S. and Subba Raju, K.: The Canadian J. Chem. Engg. **47**, 365 (1969)
5. Krishna, M. S. and Jagannadha Raju, G. J. V.: Indian J. Technol. **3**, 263 (1965).
6. Krishna, M. S., Jagannadha Raju, G. J. V. and Venkata Rao, C.: Indan J. Technol. **4**, 8 (1966)
7. Reiss, L. P. and Hanratty, T. T.: A.I.Ch.E. Journal **8**, 245 (1962)

B. Subba Rao
M. S. Krishna
G. J. V. Jagannadha Raju

Department of Chemical Engineering, Andhra University, Visakhapatnam, India